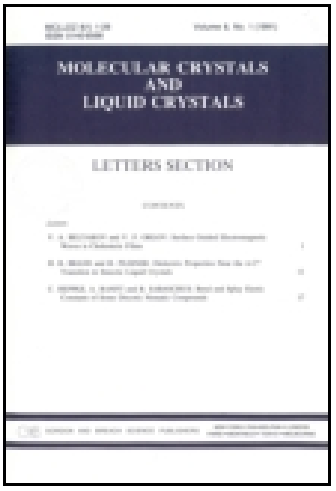

Molecular Crystals and Liquid Crystals
Publication details, including instructions for authors and subscription information:
http://www.tandfonline.com/loi/gmcl20

Characteristics of Cu_2ZnSnS_4 Thin Films Fabricated by Sulfurization of Two Stacked Metallic Layers

Sungwook Hong[a] & Chan Kim[b]
[a] Division of Science Education, Daegu University, Gyeongsan, Korea
[b] Department of Physics, Kyungpook National University, Daegu, Korea
Published online: 06 Dec 2014.

To cite this article: Sungwook Hong & Chan Kim (2014) Characteristics of Cu_2ZnSnS_4 Thin Films Fabricated by Sulfurization of Two Stacked Metallic Layers, Molecular Crystals and Liquid Crystals, 602:1, 134-143, DOI: 10.1080/15421406.2014.944751

To link to this article: http://dx.doi.org/10.1080/15421406.2014.944751

Mol. Cryst. Liq. Cryst., Vol. 602: pp. 134–143, 2014

ISSN: 1542-1406 print/1563-5287 online
DOI: 10.1080/15421406.2014.944751

Taylor & Francis
Taylor & Francis Group

Characteristics of Cu_2ZnSnS_4 Thin Films Fabricated by Sulfurization of Two Stacked Metallic Layers

SUNGWOOK HONG[1,*] AND CHAN KIM[2]

[1]Division of Science Education, Daegu University, Gyeongsan, Korea
[2]Department of Physics, Kyungpook National University, Daegu, Korea

A Cu_2ZnSnS_4 (CZTS) film was fabricated by sulfurization of two stacked layers of Cu (Zn, Sn) (CZT) alloy precursors. The sulfurization was performed in an evacuated and sealed quartz ampoule with sulfur powder, in which samples were annealed at 450°C, 500°C, or 550°C for 1 h and then allowed to cool naturally. The XRD patterns of all samples are well matched to those of the CZTS crystal. In this study, it is confirmed that the Sn in the metal precursors is lost in the form of SnS gas and a SnS_2 solid that crystallizes upon the combination of SnS and S when the CZTS film is annealed. The band gap energy of CZTS absorber was determined to be 1.370–1.414 eV. The surface morphology and grain shapes of these CZTS thin films were analyzed using SEM images and XRD patterns.

Keywords CZTS; Cu_2ZnSnS_4; solar cell; band gap energy; sulfurization; photovoltaics

Introduction

Cu_2ZnSnS_4 (CZTS) thin films are interesting materials for thin-film solar cell absorbers because of their abundant and environmentally benign constituents, high absorption coefficients ($>10^4$ cm^{-1}) in the visible range, and *p*-type electrical conductivity [1–3].

Recently, the energy conversion efficiency of CZTS-based solar cells fabricated using the vacuum process was reported to be up to 8.4% [4]. However, the theoretical energy conversion efficiency of CZTS-based solar cells is 32.2% [5]. Various methods of fabricating CZTS absorbers have been reported, such as RF-magnetron sputtering [6–7], chemical bath processes [8], electrospinning processes [9], co-evaporation [10], spray pyrolysis [11], sol-gel sulfurization [12], and so on. However, the conversion efficiencies of solar cell devices fabricated using these methods are still much lower than those of CIGS-based solar cells, as well as the theoretical conversion efficiency. To improve the conversion efficiency of CZTS-based solar cells, it is very important to understand the basic crystal structure and optical and electrical characteristics of the CZTS absorber. In this study, the radio-frequency (RF) magnetron sputtering method, which has certain advantages such as simplicity and precise

*Address correspondence to Sungwook Hong, Division of Science Education, Daegu University, Jillyang, Gyeongsan, Gyeongbuk, 712–714, Korea (ROK). E-mail: swhong@daegu.ac.kr

Color versions of one or more of the figures in the article can be found online at www.tandfonline.com/gmcl.

chemical composition control [7], was used to prepare metal precursors stacked in different orders, Cu-Sn/Zn and Zn/Cu-Sn, on Mo-coated soda glass using single-component sources of Cu, Sn, or Zn. The effects of the stacking order of the metal layers have been reported several times [13–15]. However, there are no reports on the influence that two kinds of metal precursors with the co-sputtered metal layers of Cu and Sn have on the sulfurization of the CZTS absorber in the presence of sulfur powder, to the best of our knowledge. The structural and optical properties and morphologies of CZTS absorbers produced using these stacking orders were investigated in detail.

Experimental

To grow Cu_2ZnSnS_4 crystals, the metal precursor was deposited on molybdenum (Mo)-coated soda lime glass using RF magnetron sputtering with single-component sources of copper (Cu), tin (Sn), and/or zinc (Zn). Cu and Sn were cosputtered on a Mo layer or a Zn layer, and Zn was sputtered as single layer on a Mo layer or a cosputtered Cu-Sn layer. Thus, the metal precursors were grown with two stacking orders, Cu-Sn/Zn and Zn/Cu-Sn. The energy conversion efficiency of thin-film solar cells is affected by the surface morphology of the metal precursor [16]. One method of improving the energy conversion efficiency of solar cells is to improve the surface morphology of the metal precursors. Single-crystalline Sn had a bad surface morphology for a CZTS absorber [16]. In contrast, it was reported that a Cu-Sn layer that was cosputtered from a Cu and a Sn single-component source targets had a very good surface morphology [17–18].

The Zn layer was sputtered on a Mo layer or a cosputtered Cu-Sn layer from a Zn source target with 135 W of RF-power for 30 min, and the Cu-Sn layer was cosputtered on a Mo layer or a Zn layer from a single-component source targets, Cu and Sn, with 90 W and 100 W RF-power, respectively for 30 min. The background pressure of the sputtering chamber was 6.0×10^{-7} Torr. The metal precursors were deposited under an argon gas pressure of 5.5 mTorr with a gas flow rate of 10 sccm at room temperature. Then, these metal precursors were sulfurized in quartz ampoules with an internal volume of 14–16 cm^3 that were evacuated and sealed. The ampoules, which included 3.5 mg of elemental sulfur pieces (99.999%, 6 mm pieces & smaller) obtained from CERAC and the metal precursor (12.5cm $\times$ 25.0cm), were annealed at 450, 500, or 550°C in the electrical furnace. The annealing temperature was increased from room temperature to 450, 500, or 550°C, and then the annealing temperature was maintained for 1 h. Finally, the samples were allowed to cool naturally for 12 h.

The crystal properties, surface morphologies, chemical compositions, and optical properties of the CZTS films were analyzed by X-ray diffraction (XRD, PANalytical X'pert Pro-MPD goniometer), scanning electron microscopy (SEM, Hitachi S-4200), energy dispersive X-ray spectroscopy (EDAX), and photoluminescence spectrometry (PL), respectively.

Results and Discussion

Figure 1 shows the crystal properties of two kinds of Cu_2ZnSnS_4 absorbers produced with different stacking orders of the metal precursor. Figure 1-(a) shows the crystal properties of CZTS absorbers formed by sulfurization of Cu-Sn/Zn/Mo metallic layers at annealing temperatures of 450, 500, and 550°C. The main peaks, (112), (200), (220), and (132), in the CZTS annealed at 450°C are clearly shown in Figure 1 [19]. The intensities of these peaks increased when the annealing temperature was increased. In addition, secondary phases appeared along with CZTS phase. The XRD pattern of the CZTS absorber annealed at

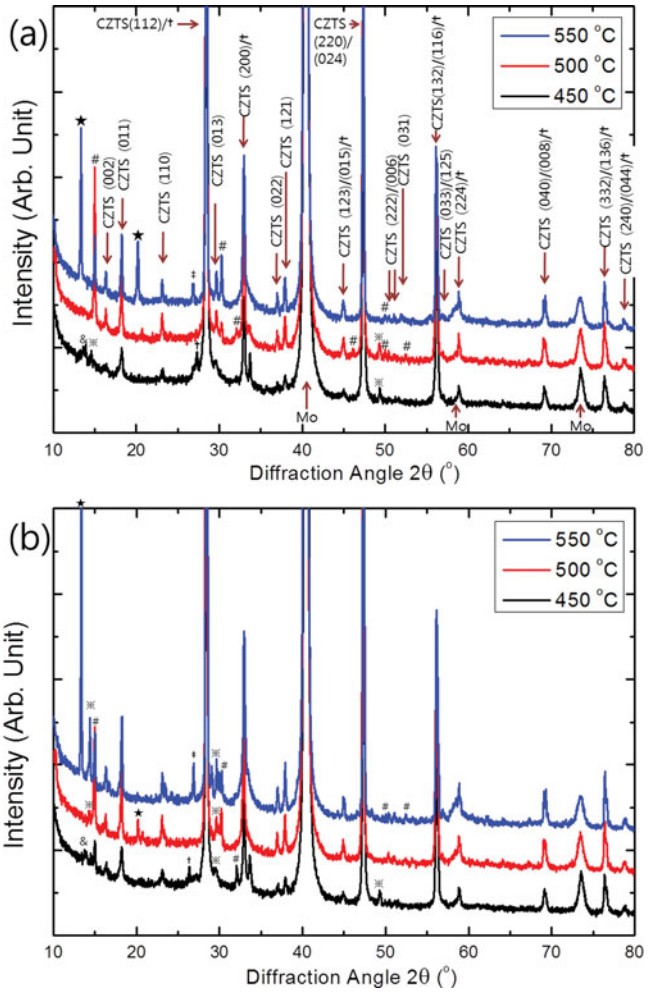

Figure 1. XRD patterns of CZTS absorbers annealed at 450, 500, and 550°C that were formed by sulfurization of (a) Cu-Sn/Zn/Mo and (b) Zn/Cu-Sn/Mo precursor on soda-lime glass. The different phase are with the symbols in parentheses as follows: $Cu_{1.83}MoS_4$ (★), SnS_2 (#), Mo_3S_4 (&), Cu_2S (†), MoS_2 (※), and ZnS (‡).

450°C shows the presence of Mo_3S_4 (marked by the & symbol), Cu_2S (†), and MoS_2 (※) phases. The peaks for Mo_3S_4 and MoS_2 show that sulfur had diffused into the Mo layer at the annealing temperature of 450°C. The Mo_3S_4 (&) peak disappeared and the MoS_2 (※) peak was enhanced in the XRD pattern of the CZTS absorber annealed at 500°C. This shows that the MoS_2 phase was more predominant than the Mo_3S_4 phase in CZTS absorbers annealed at over 500°C. The SnS_2 (#) phase also newly appeared in the XRD pattern of the CZTS absorber annealed at 500°C. The SnS_2 solid phase is created by chemical bonding of the Sn in the precursor with S that had diffused into the interior of the metal precursor. The SnS_2 solid phase decomposes into SnS (solid) and 1/2 S at high sulfur partial pressures. Then, the solid SnS changes into a gas [20]. When the ampoules cool down, the SnS (gas) was combines with S to again create SnS_2 (solid) outside of the CZTS absorber.

Table 1. Chemical compositions of the CZTS films formed by sulfurization of metallic precursors with two different stacking orders

Metal layer order	Cu-Sn/Zn/Mo			Zn/Cu-Sn/Mo		
Annealing temperature	450°C	500°C	550°C	450°C	500°C	550°C
Cu/(Zn+Sn)	1.10 ± 0.013	1.26 ± 0.082	1.20 ± 0.015	1.35 ± 0.004	1.31 ± 0.037	1.35 ± 0.018
Zn/Sn	1.01 ± 0.040	1.06 ± 0.015	1.08 ± 0.055	0.94 ± 0.007	0.97 ± 0.013	0.96 ± 0.012
S/metal	0.88 ± 0.014	0.98 ± 0.067	0.89 ± 0.022	0.86 ± 0.005	0.80 ± 0.098	0.80 ± 0.012

Therefore, SnS_2 was attached to the surface of the CZTS absorber and the interiors of the ampoules. This phenomenon causes Sn loss during the fabrication CZTS by sulfurization of a metal precursor. This phenomenon occurs during sulfurization of differently ordered Zn/Cu-Sn/Mo metal precursors, as well.

Table 1 shows the chemical composition of CZTS absorber as measured by the energy-dispersive X-ray spectrometer (EDAX). The atomic ratios were determined as the mean values for five scanning areas of 40 μm $\times$ 40 μm on the each sample. The compositional uniformity of the CZTS thin film is confirmed by the low standard deviations of the atomic ratios, as seen in Table 1. When the annealing temperature was increased, the Zn/Sn ratio also increased, because of the Sn loss during the annealing process. In the CZTS absorbers formed Zn/Cu-Sn/Mo layers by annealing at 500 and 550°C, the Zn/Sn ratios were similar, at 0.97 and 0.96. As described above, this is a result of Sn loss from the precursor during the annealing process, where the lost Sn was attached onto the surface of the CZTS absorber in the form of a SnS_2 solid.

As shown in Figure 1, the intensity of the SnS_2 (#) peaks increased when the annealing temperature was increased. The $Cu_{1.83}MoS_4$ (★) peak newly appeared in the XRD pattern of the CZTS absorbers annealed at 550°C in Figure 1-(a). This shows that S easily diffused at the high annealing temperature. Furthermore, the XRD pattern of the CZTS absorber annealed at 550°C in Figure 1–(a) shows peaks for the MoS_2 (※), SnS_2 (#), and ZnS (‡) phases.

As shown in Figure 1-(b), in the XRD pattern of the CZTS absorber formed by sulfurization of the Zn/Cu-Sn/Mo layers, the $Cu_{1.83}MoS_4$ (★) phase was already present in the CZTS absorber annealed at 500°C, and its intensity was enhanced at for the CZTS absorber annealed at 550°C, because Cu, which has a good mobility in the metal precursor [15], was located between the Zn and Mo layers. The intensity of the MoS_2 (※) peak increased more for this CZTS absorber than for the CZTS absorber fabricated from the Cu-Sn/Zn/Mo precursor.

Figure 2 and Figure 3 show SEM images of the CZTS thin films fabricated from Cu-Sn/Zn/Mo and Zn/Cu-Sn/Mo precursors, respectively. The thicknesses of all samples are about 1.5 μm. Figure 2-(c), Figure 3-(b), and Figure 3-(c) show that new layers were formed between the Mo layer and the CZTS absorber layer. These MoS_2 and $Cu_{1.83}MoS_4$ layers are produced by the penetration of sulfur into the Mo layer. When the annealing temperature was increased, the grain size was increased, which improves the energy conversion efficiency. However, the numbers of voids was also increased, which deteriorates the energy conversion efficiency, because Sn loss from the CZTS precursors to a gas state occurred during the annealing process.

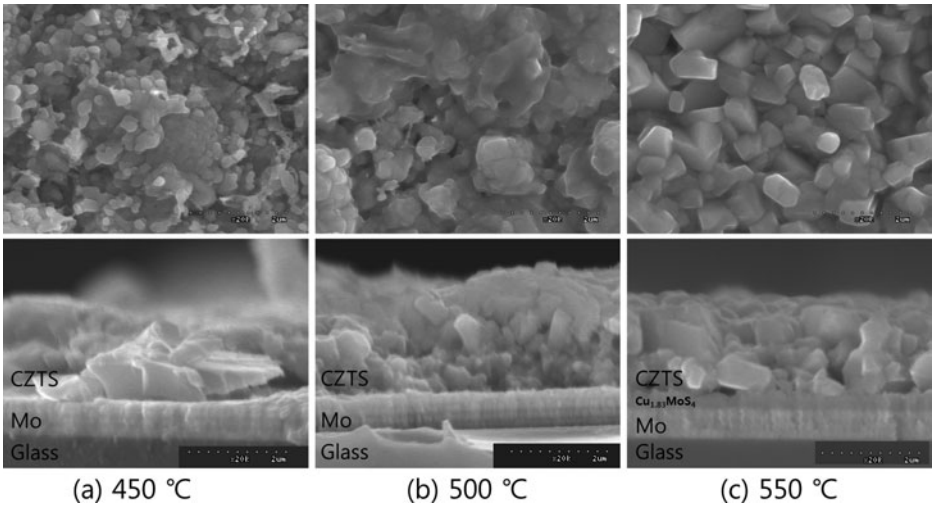

Figure 2. SEM images of the surface morphology and cross section of Cu_2ZnSnS_4 films formed by sulfurization of a Cu-Sn/Zn/Mo precursor on soda-lime glass.

Figure 4 shows the crystallite size of the CZTS thin films determined by the Scherrer formula [2, 18] as a function of annealing temperature. The (112) peaks in the XRD patterns were used to determine the crystallite sizes. As the annealing temperature is increased, the crystallite sizes increased. This result agrees well with the SEM analysis, which showed that the grain size increased as the annealing temperature increased. It is also found that the crystallite size of the CZTS absorber formed by sulfurization of the Cu-Sn/Zn/Mo precursor is larger than that of the CZTS absorber formed by sulfurization of the Zn/Cu-Sn/Mo precursor.

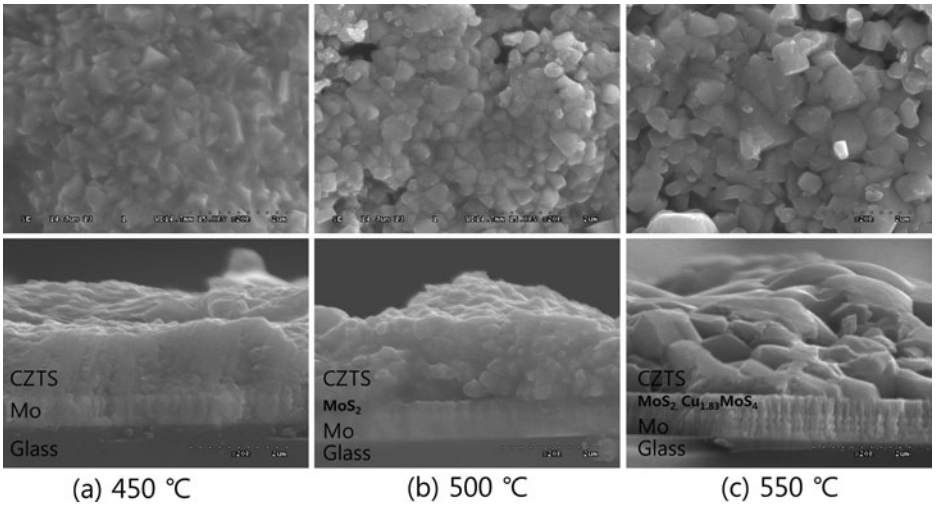

Figure 3. SEM images of the surface morphology and cross section of Cu_2ZnSnS_4 films formed by sulfurization of a Zn/Cu-Sn/Mo precursor on soda-lime glass.

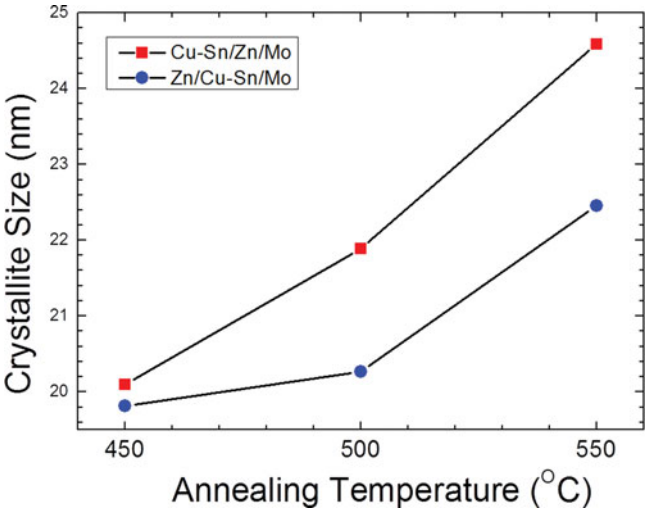

Figure 4. Changes in the crystallite size in the CZTS film formed by sulfurization of the two precursors with different metallic layer stacking orders as a function of annealing temperature.

The lattice constants of the CZTS crystals, which have a tetragonal structure, were calculated from the (112) and (220) peaks in the XRD patterns [6]. The lattice constants were determined to be $a = 5.445$ Å and $c = 10.834$ Å for both kinds of CZTS thin films. These lattice constants are similar to those of a CZTS single crystal, $a = 5.427$ Å and $c = 10.871$ Å [21]. The band gap energies of the CZTS absorbers were determined using PL spectrometer ($\lambda = 532$ nm semiconductor laser) with the same integration time. Figure 5 and Figure 6 show the PL spectra of CZTS absorbers formed by the sulfurization of Cu-Sn/Zn/Mo and Zn/Cu-Sn/Mo precursors, respectively. The PL intensity of the CZTS absorbers annealed at 550°C is higher and clearer than those of samples annealed at other temperatures, as shown in Figure 5-(a) and Figure 6-(a). The PL curve of the CZTS absorber annealed at 550°C shows a broad range for the energy band gap, because of the secondary MoS_2 and Cu_2S phases, which were confirmed by the XRD pattern. The band gaps of MoS_2 and Cu_2S single crystals were reported to 1.29 eV and 1.38 eV, respectively [22–23]. In addition, the energy band gap of the CZTS absorber was reported to 1.4–1.5eV [1]. These three semiconductors have similar band gap energy ranges. Figure 5-(b) and Figure 6-(b) show the results of Gaussian fitting with three peaks. As shown in Figure 5-(b) for the Cu-Sn/Zn/Mo precursor, the peaks of the Gaussian distributions for MoS_2, Cu_2S, and CZTS crystals appeared at 1.310, 1.353, and 1.388 eV, respectively. These values matched the band gap energy values of the corresponding single crystals well. As shown in Figure 6-(b) for the Zn/Cu-Sn/Mo precursor, the peaks of the Gaussian distributions for MoS_2, Cu_2S, and CZTS crystals appeared at 1.287, 1.343, and 1.370 eV, respectively, which are again similar with the values for single crystals and for the Cu-Sn/Zn/Mo precursor.

However, the PL intensity of the CZTS crystal is larger than those of the MoS_2 and Cu_2S crystals in Figure 5-(b), whereas the PL intensity of the Cu_2S crystal is larger than those of the MoS_2 and CZTS crystals in Figure 6-(b). This demonstrates that the CZTS domains in the CZTS absorber formed by sulfurization of the Cu-Sn/Zn/Mo precursor were more crystallized than those in the absorber formed from the Zn/Cu-Sn/Mo precursor, as described in the analysis of the crystallite size in Figure 4. The same result is confirmed

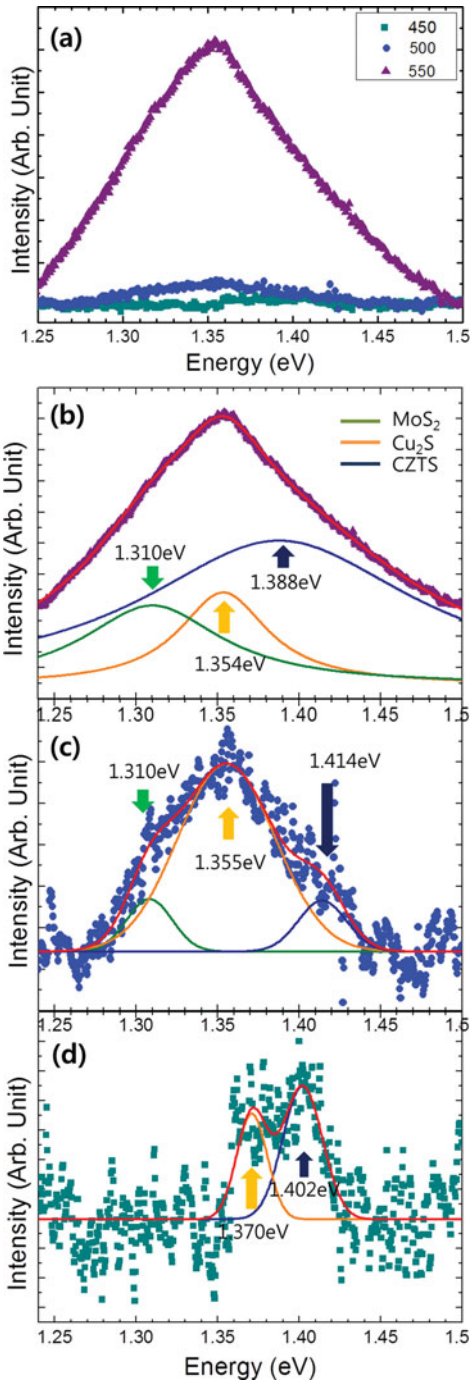

Figure 5. (a) PL curves of Cu_2ZnSnS_4 absorbers formed by sulfurization of the Cu-Sn/Zn/Mo metallic precursor at all annealing temperatures and (b–d) details of the fitting for the absorber formed at annealing temperatures of (b) 550°C, (c) 500°C, and (d) 450°C. The Gaussian fitting curves in green (left side), orange (middle), and dark blue (right side) denote the energy absorption curves for MoS_2, Cu_2S, and CZTS single crystals, respectively.

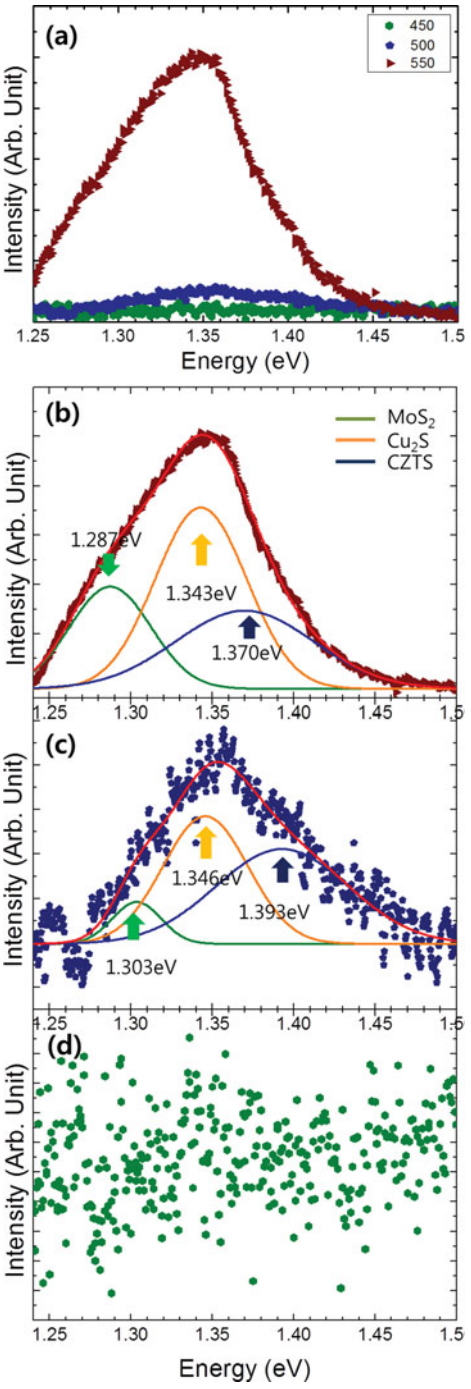

Figure 6. (a) PL curves of Cu_2ZnSnS_4 absorbers formed by sulfurization of the Zn/Cu-Sn/Mo metallic precursor at all annealing temperatures and (b–d) details of the fitting for the absorbers formed at annealing temperatures of (b) 550°C, (c) 500°C, and (d) 450°C. The Gaussian fitting curves in green (left side), orange (middle), and dark blue (right side) denote the energy curves of MoS_2, Cu_2S, and CZTS single crystals, respectively.

in Figure 5-(d) and Figure 6-(d), which show the PL data for CZTS absorber annealed at 450°C. The noise-to-signal levels in Figure 5-(d) and Figure 6-(d) are much larger than those in the other figures because of the poor crystallization of the CZTS, Cu_2S and MoS_2. Another reason for the high noise level is that the PL intensity of the CZTS absorber annealed at 450°C was measured over the same integration time as those of other CZTS absorbers. This confirms that the CZTS formed by sulfurization of the Cu-Sn/Zn/Mo precursor was more crystallized than that formed from the Zn/Cu-Sn/Mo precursor, since the CZTS absorbers were annealed at 450°C. In other words, the CZTS absorber formed from the Cu-Sn/Zn/Mo precursor was crystalized at a lower annealing temperature than was the CZTS absorber formed from the Zn/Cu-Sn/Mo precursor. This also causes the relatively higher PL intensity of CZTS crystal shown Figure 5-(b) than that in Figure 6-(b). Although the noise-to-signal ratio was large in Figure 5-(d), the band gap energies of the CZTS crystal and MoS2 crystal were estimated using a Gaussian data fitting method. The band gap energies of Cu_2S and CZTS crystals in the CZTS absorber formed by sulfurization of the Cu-Sn/Zn/Mo precursor formed at annealing temperature 450°C were determined to be 1.370 and 1.402 eV, respectively.

Conclusions

CZTS absorbers were fabricated by sulfurization of two kinds of metal precursors with Cu-Sn/Zn/Mo and Zn/Cu-Sn/Mo layer structures at different annealing temperatures of 450, 500, or 550°C in evacuated and sealed quartz ampoules. XRD analysis confirmed the presence of CZTS crystals, but some MoS_2, Cu_2S, Mo_3S_4, $Cu_{1.83}MoS_4$, ZnS, and SnS_2 secondary phases were also present. During annealing of the CZTS absorber, Sn is lost as SnS gas and a SnS_2 solid, which was coated on surfaces of the CZTS thin films and on the walls of the quartz ampules. The band gap energies of CZTS absorbers were determined to be 1.370–1.414 eV. In this study, it was confirmed that as compared to the CZTS absorber fabricated using Zn/Cu-Sn/Mo precursor, the CZTS absorber formed by sulfurization of the Cu-Sn/Zn/Mo metal precursor had better properties, including a bigger grain size, smaller amounts of secondary phases like Cu_2S, and less diffusion of Cu into the Mo. The lattice constants of all samples, which had tetragonal structures, were determined to be $a = 5.445$ Å and $c = 10.834$ Å.

Funding

This study was supported by the Daegu University Research Grant, 2013.

References

[1] Ito, K., & Nakazawa, T. (1998). *Jpn. J. Appl. Phys.*, *27*, 2094.
[2] Rajeshmon, V. G., Kartha, C. S., Vijayakumar, K. P., Sanjeeviraja, C. Abe, T. & Kashiwaba, Y. (2011). *Solar Energy*, *85*, 249.
[3] Matsushita, H. Maeda, T. Katsui, A. & Rakizawa, T. (2000). *J. Cryst. Growth*, *208*, 416.
[4] Shin, B. Gunawan, O. Zhu, Y. & Bojarczuk, N. A. (2013). *Prog. Photovoltaics Res. Appl.*, *21*, 72.
[5] Shockley, W. & Queisser, H. J. (1961). *J. Appl. Phys.*, *32*, 510.
[6] Kim, C. & Hong, S. (2013). *Mol. Cryst. Liq. Cryst.*, In-press.
[7] Wang, J. Li, S. Cai, J. B. shen, Ren, Y. & Qin, G. (2013). *J. Alloys Comp.*, *552*, 418
[8] Cao, M. Li, L. Zhang, B. L., Huang, J. Wang, L. J., Shen, Y. Sun, Y. & Jiang, J. C. (2013). *Sol. Energy Mater. Sol., Cells 117*, 81.

[9] Chen, L. & Chuang, Y. (2013). *J. Power Sources. 241*, 259.
[10] Tanaka T. Yoshida, A. Saiki, D. Saito, K. Guo, Q. Nishio, M. & Yamaguchi, T. (2010). *Thin Solid Films*, *518*, S29.
[11] Kumar, Y. B. K., Babu, G. S., Bhaskar, P. U., & Raja, V. S. (2009). *Sol. Energy Mater. Sol. Cell*, *93*, 1230.
[12] Tanaka, K. Onuki, M. Moritake, N. & Uchiki, H. (2009). *Sol. Cell*, *93*, 583.
[13] Yoo, H. & Kim, J. (2010). *Thin Solid Films*, *518*, 6567.
[14] Araki, H. Mikaduki, A. Kubo, Y. Sata, T. Jimbo, K. Maw, W. S., Katagiri, H. Yamazaki, M. Oishi, K. & Takeuchi, A. (2008). *Thin Solid Films*, *517*, 1457.
[15] Fernandes, P. A., Salome, P. M. P., & Cunha, A. F. (2009). *Semicond. Sci. Technol.*, *24*, 105013.
[16] Katagiri, H. (2005). *Thin Solid Films*. *426*, 480–481.
[17] Hong, S. (2012). *Mol. Cryst. Liq. Cryst.*, *565*, 153.
[18] Hong, S. Kim, C. Park, S. C., Rhee, I. Kim, D. H., & Kang, J. K. (2012). *Mol. Cryst. Liq. Cryst.*, *565*, 147.
[19] Menchetti, S. Bernardini, G. P., Bindi, L. & Bonazzi, P. (2003). *Canadian Mineralogist*, *41*, 639.
[20] Redinger, A. Berg, D. M., Dale, P. J., & Siebentritt, S. (2011). *J. Am. Chem. Soc.*, *133*, 3320.
[21] Hall, S. R., Szymanski, J. T., & Stewart, J. M. (1978). *Can. Mineral.*, *16*, 131.
[22] Mak, K. F., Lee, C. Hone, J. Shan, J. & Heinz, T. F. (2010). *Phys. Rev. Lett.*, *105*, 136805.
[23] Connor, S. T., Hsu, C. Weil, B. D., Aloni, S. & Cui, Y. (2009). *J. Am. Chem. Soc.*, *131*, 4962.